The Canadian Mineralogist
Vol. 48, pp. 17-28 (2010)
DOI: 10.3749/canmin.48.1.17

ROUMAITE, $(Ca,Na,\square)_3(Ca,REE,Na)_4(Nb,Ti)[Si_2O_7]_2(OH)F_3$, FROM ROUMA ISLAND, LOS ARCHIPELAGO, GUINEA: A NEW MINERAL SPECIES RELATED TO DOVYRENITE

CRISTIAN BIAGIONI[§]

Dipartimento di Scienze della Terra, Università di Pisa, Via Santa Maria 53, I–56126 Pisa, Italy

ELENA BONACCORSI

Dipartimento di Scienze della Terra, Università di Pisa, Via Santa Maria 53, I–56126 Pisa, Italy and Istituto di Geoscienze e Georisorse, CNR, Via Moruzzi 1, I–56100 Pisa, Italy

STEFANO MERLINO

Dipartimento di Scienze della Terra, Università di Pisa, Via Santa Maria 53, I–56126 Pisa, Italy

GIAN CARLO PARODI

Unité Minéralogie–Pétrologie (USM 201) and CNRS UMR 7160, Muséum National d'Histoire Naturelle, 61 rue Buffon, F–75005 Paris, France

NATALE PERCHIAZZI

Dipartimento di Scienze della Terra, Università di Pisa, Via Santa Maria 53, I–56126 Pisa, Italy

VINCENT CHEVRIER

Unité Minéralogie–Pétrologie (USM 201) and CNRS UMR 7160, Muséum National d'Histoire Naturelle, 61 rue Buffon, F–75005 Paris, France

DANILO BERSANI

Dipartimento di Fisica, Università di Parma, Viale G.P. Usberti 7/a, I–43100 Parma, Italy

ABSTRACT

Roumaite, $(Ca,Na,\square)_3(Ca,REE,Na)_4(Nb,Ti)[Si_2O_7]_2(OH)F_3$, a new mineral species, occurs as a late-stage product in cavities of peralkaline nepheline syenites on Rouma Island, in the Los Archipelago, in Guinea; associated minerals are aegirine, albite, analcime, arfvedsonite, catapleiite, a eudialyte-group member, microcline, sodalite, sphalerite, steacyite and villiaumite. Roumaite is monoclinic, space group *Cc*, with cell parameters *a* 7.473(2), *b* 11.294(2), *c* 18.778(4) Å, β 101.60(2)°, *V* 1552.5(6) Å^3, *Z* = 4. The modular structure of roumaite consists of stacks of tobermorite-like layers, "octahedral" layers and disilicate groups; it is closely related to dovyrenite.

Keywords: roumaite, new mineral species, modular structure, OD character, agpaitic syenite, Los Archipelago, Guinea.

SOMMAIRE

La roumaïte, $(Ca,Na,\square)_3(Ca,REE,Na)_4(Nb,Ti)[Si_2O_7]_2(OH)F_3$, espèce minérale nouvelle, a été découverte dans des cavités de syénites néphéliniques hyperalcalines de l'île de Rouma, complexe magmatique de l'archipel de Los, en Guinée. Lui sont associés aegyrine, albite, analcime, arfvedsonite, catapléiite, un membre du groupe de l'eudialyte, microcline, sodalite, sphalérite,

§ *E-mail address*: biagioni@dst.unipi.it

steacyite et villiaumite. La roumaïte est monoclinique, groupe spatial *Cc*, avec paramètres réticulaires *a* 7.473(2), *b* 11.294(2), *c* 18.778(4) Å, β 101.60(2)°, *V* 1552.5(6) Å^3, *Z* = 4. La structure modulaire de la roumaïte est faite d'empilements de couches semblables à la tobermorite, des couches d'octaèdres et des groupes disilicatés; cette espèce a des liens proches avec la dovyrénite.

(Traduit par la Rédaction)

Mots-clés: roumaïte, nouvelle espèce minérale, structure modulaire, caractère OD, syénite agpaïtique, archipel de Los, Guinée.

Introduction

The Los Archipelago is located 5 km offshore of Conakry, capital of Guinea. The islands represent the outcrops of a peralkaline complex formed by nepheline syenites emplaced in the West African continental margin during Albian time (104.3 ± 1.7 Ma; Moreau *et al.* 1996). In this complex, Moreau *et al.* (1996) distinguished an agpaitic and a miaskitic suite. The agpaitic syenite is enriched in incompatible and volatile elements, and in interesting rare minerals, such as Zr–Ti–Nb–REE disilicates belonging to the cuspidine and rinkite families, whereas the miaskitic one is enriched in augite, hastingsite, zircon, and titanite. As part of the SYNTHESYS European project, we investigated a suite of samples from the Los Archipelago kept in the Muséum National d'Histoire Naturelle of Paris, paying particular attention to a specimen tentatively identified as nacareniobsite-(Ce) by Parodi & Chevrier (2004). Single-crystal X-ray-diffraction studies performed on this specimen, together with electron-microprobe analyses, allowed us to identify this material as a new mineral species. The mineral and its name were approved by IMA–CNMNC (IMA 2008–024). The mineral is named *roumaite* after the type locality, Rouma Island, located in the central lagoon of Los Archipelago, where the specimen was found. Although roumaite shows the presence of a high content of REE, the low quality of the intensity data related to the widespread structural disorder does not allow us to assess a highly reliable distribution of these elements and to definitely infer the presence of a REE-dominant site or sites; for this reason, the Levinson suffix (Levinson 1966, Bayliss & Levinson 1988) is not used for the time being.

Holotype material is deposited in the Muséum National d'Histoire Naturelle, 61, rue Buffon, F–75005 Paris, France, catalogue # MNHN208.1; cotype material is deposited in the mineralogical collection of Museo di Storia Naturale e del Territorio, Università di Pisa, Via Roma 79, Calci (PI), Italy, catalogue # 18873.

Mineralogical Characterization

Appearance and physical properties

Roumaite is very rare; only a few crystals could be identified. It occurs as very small acicular crystals up to 0.5 mm in length, colorless and transparent, with a silky luster, elongate on [100] (Fig. 1). Rarely, it occurs as specimens tabular on (001), formed by parallel growth of acicular individuals. The streak is white. Roumaite is brittle; it is not fluorescent under ultraviolet light. Hardness and density could not be measured because of the small size of the crystals; the calculated density, based on the empirical formula, is 3.33 g/cm^3.

Owing to the very small size of the crystals, it was possible to measure only some of the optical properties of roumaite. The crystals are colorless, nonpleochroic; the indices of refraction parallel to the elongation of the crystals (corresponding to the [100] direction) and in a direction normal to [100], are, in both cases, between 1.652 and 1.654. The measured maximum angle of extinction is about 4° on [001]; the elongation is positive, and the birefringence is weak. The compatibility index is –0.007 (superior) (Mandarino 1981).

Roumaite is a late-stage product of hydrothermal activity in the cavities of nepheline syenites and is associated with aegirine, albite, analcime, arfvedsonite, catapleiite, a phase of the eudialyte group, microcline, sodalite, sphalerite, steacyite, and villiaumite.

Chemical analyses

In order to verify the homogeneity of the material and to check the elements to be sought during our electron-microprobe investigation, qualitative chemical analyses were performed using SEM–EDS equipment. The crystals of roumaite seem to be homogeneous.

Quantitative chemical analyses were performed using a JEOL JXA–8600 electron microprobe, operating in wavelength-dispersion mode; the voltage was 15 kV, the beam current was 20 nA, and the beam diameter was 5 μm. We used the following standards: kaersutite (Si*K*α, Ca*K*α, Fe*K*α), albite (Na*K*α), ilmenite (Ti*K*α), monazite (Ce*L*α, La*L*α, Pr*L*β, Nd*L*β), cubic zirconia (Zr*L*α, Y*L*α), metallic niobium (Nb*L*α), bustamite (Mn*K*α), metallic thorium (Th*L*α), and fluorite (F*K*α). Corrections were calculated according to the ZAF procedure. The composition of roumaite, based on average results of six analyses, is given in Table 1.

Notwithstanding the fairly high number of measured elements, the analyses showed consistently low totals, between about 94 and 99 wt%, with a mean value of about 96.6 wt%. Such low values could be an analytical artefact, due to the pronounced acicular shape of the

Fig. 1. Acicular crystals, up to 0.5 mm, of roumaite, with black prisms of aegirine.

roumaite crystals (10 μm in diameter) very close to the nominal diameter of the electron beam, or they could be related to the presence of H_2O in the structure.

In order to verify the latter hypothesis, non-polarized micro-Raman spectra were obtained in nearly back-scattered geometry with a Jobin–Yvon Horiba "Labram" apparatus, equipped with a motorized *x–y* stage and an Olympus microscope with a ×50 objective. The 632.8 nm line of an He–Ne laser was used; laser power was controlled by means of a series of density filters. The minimum lateral and depth resolution was set to a few μm. The system was calibrated using the 520.6 cm^{-1} Raman band of silicon before each experimental session. Spectra were collected with multiple acquisitions (2 to 6) with single counting times ranging between 20 and 180 seconds. The Raman spectra show the important contributions of fluorescence effects related to the presence of REE, which does not allow an accurate study of the region between 3000 and 3800 cm^{-1} in which the stretching vibrations of O–H bonds should be located. In order to try to avoid the fluorescence emission in the OH-stretching region, a second series of Raman spectra was acquired using a different excitation line (488 nm) on a Horiba Jobin–Yvon T64000 apparatus equipped with an argon laser. Unfortunately, in this case also the region between 3000 and 3800 cm^{-1} was hindered by strong fluorescence bands. In the spectral region typical of OH-bending vibrations (1500–1700 cm^{-1}), only a weak band at 1582 cm^{-1} is present, but it is very broad (nearly 100 cm^{-1} at FWHM). It does not provide a sure sign of presence of H_2O. Therefore, it was not possible to confirm or exclude the presence of H_2O using Raman spectroscopy.

TABLE 1. THE COMPOSITION OF ROUMAITE

Oxides	wt.%	range	Atoms*	*apfu*
SiO_2	29.78	28.68 – 31.32	Si^{4+}	4
TiO_2	2.91	2.57 – 3.43	Ti^{4+}	0.29
ZrO_2	0.02	0.00 – 0.09	Zr^{4+}	0.00
ThO_2	0.07	0.00 – 0.33	Th^{4+}	0.00
Y_2O_3	0.67	0.41 – 0.80	Y^{3+}	0.05
Ce_2O_3	13.15	11.97 – 13.67	Ce^{3+}	0.65
La_2O_3	5.02	4.37 – 5.40	La^{3+}	0.25
Nd_2O_3	2.28	1.97 – 2.51	Nd^{3+}	0.11
CaO	20.61	19.58 – 21.30	Ca^{2+}	2.97
FeO	n.d.		Fe^{2+}	0.00
MnO	0.02	0.00 – 0.05	Mn^{2+}	0.00
Na_2O	7.83	6.69 – 9.43	Na^{+}	2.04
Nb_2O_5	10.51	8.63 – 11.27	Nb^{5+}	0.64
F	6.46	5.78 – 7.25	F^{-}	2.75
Sum	99.33	97.22 – 101.26		
O = F	-2.72			
Total	96.61			

The composition reported is the average results of six electron-microprobe analyses (six points). * The crystal-chemical content in the last column is calculated on the basis of Si = 4 *apfu*.

The empirical formula of roumaite, calculated from chemical data on the basis of four Si atoms per

formula unit, is $(Ca_{2.97}Na_{2.04}Ce_{0.65}La_{0.25}Nd_{0.11}Y_{0.05})_{\Sigma 6.07}(Nb_{0.64}Ti_{0.29})_{\Sigma 0.93}(Si_2O_7)_2F_{2.75}O_{0.38}$. The low total of the "octahedral" cations (7.00 *apfu* instead of the theoretical 8 *apfu*) for a mineral of the rinkite group (see below) and the low total of anions (17.13 *apfu* instead of 18 *apfu*) suggest the possible presence of partially vacant sites (as in dovyrenite), and some H_2O as $(OH)^-$ groups. In the above formula, the introduction of 0.38 H_2O led to 0.76 $(OH)^-$ *pfu*, corresponding to ~0.85 wt% H_2O.

The simplified formula of roumaite could be written as $(Ca,Na,REE,\square)_{\Sigma 7.00}(Nb,Ti)(Si_2O_7)_2(OH)F_3$.

X-ray crystallography

The X-ray powder-diffraction pattern was collected using a Gandolfi camera 114.6 mm in diameter with Cu$K\alpha$ radiation; this pattern is very similar to those of other phases of the rinkite group, such as rinkite, nacareniobsite-(Ce), and mosandrite. In Table 2, we present the observed X-ray powder pattern of roumaite; indexing was made taking into account the intensities of reflections measured during the single-crystal data collection.

Remarkably, single-crystal oscillation and Weissenberg photographs showed a doubling of the *b* cell parameter (11.3 Å instead of 5.6 Å) with respect to the minerals of the rinkite group. Through these observations, it was possible to define a preliminary unit-cell ($a \approx 7.5$, $b \approx 11.3$, $c \approx 18.8$ Å, $\beta \approx 101.5°$) and to establish *C*2/*c* or *Cc* as possible space-groups.

As is found in the related mineral rinkite (Ferraris *et al.* 2008), roumaite also presents order–disorder (OD) character: all the reflections with *k* odd values (and also with *h* odd values, owing to the *C* centering) are very weak and display diffuseness along **c***. The "family cell" corresponding to the strong and sharp reflections (even values of *k* and *h*) displays an orthorhombic symmetry: $a_F \approx 3.75$, $b_F \approx 5.65$, $c_F \approx 18.5$ Å, space-group symmetry *Pmnn* (or *P*2*nn*). The diffuseness of the weak reflections ("characteristic reflections") depends on the OD nature of the mineral. At this point, it seems proper to mention the close correspondence with the unit-cell data and space-group symmetry given by Kadiyski *et al.* (2008) for dovyrenite, $Ca_6Zr[Si_2O_7]_2(OH)_4$, taking into consideration the different choice of the reference unit-cell: $a_D = 5.67$, $b_D = 18.70$, $c_D = 3.73$ Å, space group *Pnnm*.

TABLE 2. X-RAY POWDER DATA FOR ROUMAITE

d_{obs}	I_{obs}	d_{calc}	*h k l*	d_{obs}	I_{obs}	d_{calc}	*h k l*
9.167	15	9.197	0 0 2			2.024	$\bar{2}$ 4 5
5.389	9.8	5.398	0 2 1	2.021	67.7	2.022	2 4 3
4.138	18.5	4.154	0 2 3			2.011	2 2 8
3.562	24.5	3.566	0 2 4	2.004	32.5	2.007	2 2 6
3.082	3.6	3.082	0 2 5	1.922	10	1.922	$\bar{1}$ 5 5
		3.073	$\bar{2}$ 2 2			1.868	$\bar{4}$ 0 2
3.057	100	3.071	2 2 0	1.846	30.2	1.852	$\bar{2}$ 2 9
		3.066	0 0 6			1.848	1 1 9
2.975	6.9	-	-	1.838	5.7	1.816	$\bar{2}$ 4 7
2.937	31.4	2.952	$\bar{2}$ 2 3	1.747	4.6	1.749	0 2 10
		2.950	2 2 1	1.707	12.9	1.711	$\bar{2}$ 4 8
2.790	40.1	2.791	0 4 1			1.709	2 4 6
2.689	46.4	2.699	0 4 2	1.680	60.1	1.681	$\bar{2}$ 6 1
		2.694	0 2 6			1.676	0 6 5
2.608	19.9	2.624	$\bar{2}$ 0 6			1.541	0 4 10
		2.619	2 0 4	1.530	14.5	1.537	$\bar{4}$ 2 8
2.567	44.4	2.578	2 2 3			1.534	4 2 4
		2.566	0 4 3	1.475	9.7	1.475	$\bar{2}$ 6 7
2.406	7.2	2.406	0 4 4			1.473	2 6 5
2.295	11.5	2.299	0 0 8	1.424	8.6	1.408	0 8 1
		2.189	$\bar{2}$ 4 3	1.267	12.7	1.268	$\bar{2}$ 4 13
2.184	30.4	2.187	$\bar{2}$ 2 7			1.267	2 4 11
		2.183	2 4 1			1.250	0 6 11
2.141	9.1	2.147	2 2 5	1.246	30.3	1.248	$\bar{4}$ 6 7
2.112	16.5	2.115	2 0 6			1.247	4 6 3
		2.114	$\bar{2}$ 4 4, 2 4 2				

A crystal of roumaite measuring about 0.4 × 0.1 × 0.1 mm^3 was mounted on a SIEMENS P4 four-circle diffractometer, and data were collected with Mo$K\alpha$ radiation ($\lambda = 0.71073$ Å). Initially, the family cell was refined using a set of 25 reflections; the parameters of the true cell were obtained through the transformation: $\mathbf{a} = 2\,\mathbf{a}_F$; $\mathbf{b} = 2\,\mathbf{b}_F$; $\mathbf{c} = \mathbf{c}_F - \mathbf{a}_F$. As every attempt to solve the structure in the space group *C*2/*c* was unsuccessful, a structure solution was attempt by direct methods (SIR–92; Altomare *et al.* 1994) in space group *Cc*. The subsequent refinement [$R_1 = 0.156$ for 943 reflections with $F_o > 4\sigma(F_o)$ and 0.20 for all the 1293 independent reflections], performed using SHELX–97 (Sheldrick 1997), showed the main features of the structure.

Owing to both the small size of the crystal and the weakness of the "characteristic reflections" (those with $k = 2n + 1$), a new set of intensity data was collected at the XRD1 beamline of the Elettra Laboratory of Basovizza (Trieste), using synchrotron radiation with $\lambda = 0.7001$ Å; a total of 120 frames (frame width 3° in ϕ) was collected using a MAR CCD detector with a diameter of 165 mm, located 36 mm from the sample. Using the HKL software (Otwinowsky & Minor 1997), we refined the cell parameters and extracted the reflection intensities. Starting from the preliminary structural model mentioned previously, a new refinement based on synchrotron data was carried out in the space group *Cc*, with cell parameters *a* 7.473(2), *b* 11.294(2), *c* 18.778(4) Å, β 101.60(2)°. The structure refinement yielded a final $R_1 = 0.086$ for 4558 independent reflections with $|F_o| \geq 4\sigma F_o$ and 0.096 for all 5292 data. All cations were refined anisotropically, whereas anions were refined only isotropically. Table 3 summarizes the details concerning the data collection and crystal-structure refinement. As suggested by the OD character of the compound (see following section), the presence of twinning by pseudomerohedry (twin axis [100] and obliquity 0.12°) was accounted for using the "TWIN 100 0$\bar{1}$0 $\bar{1}$01" instruction in SHELX–97 (Sheldrick 1997). The refined ratio of the twins is about 0.5.

The presence of reflections not assignable to roumaite was detected in the data collected at the Elettra Laboratory; these reflections could be indexed on the

basis of a rinkite-like cell, pointing to the presence of rinkite-like domains inside roumaite crystals. As pointed out by Ferraris *et al.* (2008), rinkite displays OD character and presents a family cell with space group and parameters coincident with those of roumaite. Consequently, the rinkite-like domains contribute to the intensities of the family reflections of the largest domains of roumaite. Taking into account this contribution, as well as that due to the presence of disordered domains, highlighted by the marked diffuseness of the characteristic reflections, distinct scale-factors were introduced for the family reflections and the characteristic reflections during the refinement of the crystal structure of roumaite.

The refined atomic parameters are listed in Table 4; the geometrical features of the coordination polyhedra are shown in Tables 5–7. The bond-valence balance is reported in Table 8. Anisotropic displacement parameters (Table 9) and a list of the structure factors (Table 10) may be obtained from the Depository of Unpublished Data, on the MAC site [document Roumaite CM48_17].

Crystal Structure

Description of the crystal structure

The roumaite structure (Fig. 2) can be described as being composed of distinct modules: a tobermorite-like layer (Merlino *et al.* 1999) and an "octahedral" layer with attached disilicate groups, both parallel to (001).

The tobermorite-like layer (Fig. 3), already described by Hoffmann & Armbruster (1997) and Merlino *et al.* (2000), consists of columns running along **a**, made of four independent edge-sharing seven-fold coordinated polyhedra. They present a pyramidal part on one side and a dome-like one on the other. The columns are connected along **b** in such a way that adjacent columns present the "capping" ligands of the pyramidal part on opposite sides of the layer, giving rise to an undulating **a**, **b** sheet. In minerals of the tobermorite group, these sites are occupied by Ca; the results of the structural study and the bond-valence balance (Table 8), calculated with the parameters given by Brese & O'Keeffe (1991), indicate that in roumaite, Ca is partially replaced by REE and Na through the substitution $2Ca^{2+} = Na^{+} + REE^{3+}$. The *M5* site is probably a Ce-dominant site, with minor replacement of Na. The occupancies of

TABLE 4. SITE OCCUPANCIES, FINAL POSITIONS, EQUIVALENT OR ISOTROPIC DISPLACEMENT PARAMETERS FOR ATOMS IN ROUMAITE

Site	Refined occupancy	*x*	*y*	*z*	U_{eq} or U_{iso}
M1	$Nb_{0.55}Ti_{0.45}$	0.7354(5)	0.6274(2)	0.9769(2)	0.0258(5)
M2	$Ca_{0.45}Na_{0.30}\square_{0.25}$	0.7429(17)	0.8755(6)	0.4796(4)	0.0189(8)
M3	$Ca_{0.60}Na_{0.15}\square_{0.25}$	0.9903(15)	0.8751(5)	0.9799(4)	0.0279(12)
M4	$Na_{0.60}Ca_{0.35}\square_{0.05}$	0.9896(15)	0.3753(5)	0.9803(4)	0.0276(12)
M5	$Ce_{0.60}Na_{0.40}$	0.6436(3)	0.7056(1)	0.2894(1)	0.0084(3)
M6	$Ca_{0.65}Ce_{0.175}Na_{0.175}$	0.3355(6)	0.4524(1)	0.1683(1)	0.0046(4)
M7	$Ca_{0.66}Ce_{0.17}Na_{0.17}$	0.6390(8)	0.7938(2)	0.7862(2)	0.0086(4)
M8	$Ca_{0.45}Ce_{0.275}Na_{0.275}$	0.3338(4)	0.9550(1)	0.1708(1)	0.0046(4)
Si1	Si	0.0832(12)	0.6998(3)	0.1176(2)	0.0168(13)
Si2	Si	0.5215(9)	0.7005(3)	0.1184(2)	0.0075(10)
Si3	Si	0.8807(9)	0.9544(3)	0.3398(3)	0.0095(10)
Si4	Si	0.4477(11)	0.9530(3)	0.3400(3)	0.0147(13)
O1	O	0.3946(28)	0.6559(12)	0.7917(7)	0.0223(22)
O2	O	0.3930(24)	0.0751(10)	0.3004(6)	0.0159(20)
O3	O	0.6765(23)	0.9457(9)	0.3610(6)	0.0189(22)
O4	O	0.5184(22)	0.5526(11)	0.9189(7)	0.0180(24)
O5	O	0.0910(17)	0.5879(6)	0.1700(4)	0.0004(13)
O6	O	0.3849(26)	0.8425(11)	0.2924(6)	0.0200(26)
O7	O	0.3983(22)	0.5767(9)	0.3017(5)	0.0129(18)
O8	O	0.2962(22)	0.7023(9)	0.0966(7)	0.0208(22)
O9	O	0.5932(17)	0.8167(7)	0.1680(4)	0.0022(13)
O10	O	0.3917(24)	0.9498(11)	0.4199(8)	0.0224(28)
O11	O	0.0883(18)	0.8165(7)	0.1659(5)	0.0042(13)
O12	O	0.9555(16)	0.6962(8)	0.0384(5)	0.0068(17)
O13	O	0.5778(16)	0.6972(8)	0.0400(5)	0.0086(18)
O14	O	0.5960(17)	0.5898(6)	0.1718(4)	0.0014(13)
F1	(F,OH)	0.7657(19)	0.4775(8)	0.0397(5)	0.0176(17)
F2	(F,OH)	0.7031(21)	0.7061(8)	0.4160(5)	0.0154(16)
F3	(F,OH)	0.7018(19)	0.7689(7)	0.9140(5)	0.0164(16)
F4	(F,OH)	0.2697(20)	0.4544(8)	0.0397(5)	0.0148(17)

TABLE 3. DATA ON CRYSTAL, DATA COLLECTION, AND STRUCTURE REFINEMENT OF ROUMAITE

Dimensions	0.1 × 0.05 × 0.05 mm³
Space group	*Cc*
Unit cell	*a* 7.473(2), *b* 11.294(2), *c* 18.778(4) Å, β 101.60(2)°
Wavelength	0.7001 Å
Detector to sample distance	36 mm
Maximum observed 2θ	65.29°
Resolution	0.65 Å
Rotation width per frame	3°
R_{int}	0.0475
Unique reflections	5292
$I > 2\sigma(I)$	4558
R_1	0.0861
wR_2	0.2432
Goodness of fit	0.904
Number of refined parameters	191

TABLE 5. BOND DISTANCES (Å) IN ROUMAITE: THE TOBERMORITE-LIKE SHEET

M5	- F2	2.320(15)	*M6*	- F4	2.366(9)
	- O2	2.353(16)		- O9	2.371(12)
	- O7	2.388(15)		- O5	2.389(12)
	- O1	2.436(18)		- O11	2.442(12)
	- O6	2.486(17)		- O14	2.480(11)
	- O14	2.530(8)		- O1	2.578(13)
	- O9	2.563(8)		- O7	2.828(10)
average		2.439	average		2.493
M7	- F3	2.367(9)	*M8*	- O14	2.343(12)
	- O6	2.382(18)		- O11	2.398(12)
	- O7	2.399(15)		- F1	2.424(9)
	- O2	2.417(16)		- O5	2.441(11)
	- O1	2.418(19)		- O9	2.498(12)
	- O5	2.522(8)		- O6	2.574(12)
	- O11	2.541(8)		- O2	2.743(10)
average		2.435	average		2.489

the *M*6–*M*8 sites were refined taking into account the above-mentioned scheme of substitution, the measured scattering power at the sites, and the achievement of sound displacement-parameters.

The "octahedral" sheets (Fig. 4) consist of two distinct columns of edge-sharing polyhedra running along **a**. A first column contains *M*2 eight-fold polyhedra alternating with small *M*1 octahedra occupied by Nb and Ti. The other column is formed by alternating *M*3 and *M*4 octahedra. Disilicate groups are attached to the *M*2 polyhedra, the largest polyhedra in the roumaite structure, on both sides of the sheet. The structural study indicated that the *M*1 site is actually occupied in the proportions Nb 55% and Ti 45%. The occupancies of the *M*2–*M*4 sites were refined taking into account the following constraints: presence of partially empty sites, as suggested by the chemical data, the scattering power at the site positions, the bond-valence balance, and the achievement of reliable anisotropic-displacement parameters. Sites *M*2 and *M*3 are partially vacant, with occupancy ($Ca_{0.45}Na_{0.30}\square_{0.25}$) and ($Ca_{0.60}Na_{0.15}\square_{0.25}$), respectively, whereas *M*4 has only a small deficiency in cations, if any, with a refined occupancy ($Na_{0.60}Ca_{0.35}\square_{0.05}$). The *M*1 octahedron is the smallest polyhedron, with an average bond-length of 1.98 Å. Whereas in other Zr–Ti–Nb disilicates, such those belonging to the cuspidine family, Nb (and Ti) distort the octahedron (*e.g.*, in wöhlerite, with a difference of 0.42 Å between the longest and shortest bond-distances: Mellini & Merlino 1979), in roumaite, as well as in the other rinkite-group minerals (rinkite: Galli & Alberti 1971, Sokolova & Hawthorne 2008, mosandrite: Bellezza *et al.* 2009), the octahedron is quite regular. In the analogous *M*1 site of rinkite (Galli & Alberti 1971) and nacareniobsite-(Ce) (Sokolova & Hawthorne 2008), bond lengths range between 1.98 and 2.02 Å, and between 1.99 and 2.03 Å, respectively. Also, in mosandrite, studied by Bellezza *et al.* (2009), the *M*1 sites are

TABLE 6. BOND DISTANCES (Å) IN ROUMAITE: THE "OCTAHEDRAL" SHEET

*M*1	- O10	1.943(15)	*M*2	- F2	2.216(11)
	- O4	1.954(14)		- F4	2.243(11)
	- O12	1.969(11)		- O3	2.321(14)
	- F3	1.974(9)		- O8	2.325(14)
	- O13	1.993(11)		- O13	2.662(18)
	- F1	2.049(9)		- O4	2.672(21)
average		1.980		- O12	2.728(18)
				- O10	2.769(22)
			average		2.492
*M*3	- O12	2.339(11)	*M*4	- O10	2.320(15)
	- O4	2.339(14)		- O13	2.332(11)
	- F4	2.350(16)		- F4	2.342(17)
	- F2	2.361(15)		- F2	2.418(16)
	- F1	2.430(16)		- F1	2.475(15)
	- F3	2.558(16)		- F3	2.511(15)
average		2.396	average		2.400

TABLE 7. BOND DISTANCES (Å) AND *T*–O–*T* ANGLES (°) IN ROUMAITE: THE DISILICATE GROUPS

Si1	- O11	1.596(9)	Si2	- O13	1.611(11)
	- O5	1.596(8)		- O14	1.629(9)
	- O12	1.599(11)		- O9	1.636(9)
	- O8	1.715(17)		- O8	1.650(16)
average		1.626	average		1.632
Si3	- O1	1.555(14)	Si4	- O6	1.551(13)
	- O7	1.574(11)		- O2	1.581(12)
	- O4	1.630(14)		- O10	1.639(16)
	- O3	1.655(17)		- O3	1.678(17)
average		1.604	average		1.612
Si1 – O8 – Si2		152.8(8)	Si3 – O3 – Si4		152.3(8)

TABLE 8. BOND-VALENCE BALANCE (*vu*) IN ROUMAITE

	O1	O2	O3	O4	O5	O6	O7	O8	O9	O10	O11	O12	O13	O14	F1	F2	F3	F4	$\Sigma_{cations}$
*M*1				0.80						0.82		0.77	0.72		0.55		0.67		4.33
*M*2			0.24	0.10				0.24		0.07		0.08	0.10			0.22		0.23	1.28
*M*3				0.25								0.25			0.15	0.18	0.11	0.19	1.13
*M*4										0.28			0.27		0.13	0.15	0.12	0.19	1.14
*M*5	0.35	0.44				0.31	0.40		0.25					0.27		0.35			2.37
*M*6	0.20				0.34		0.10		0.35		0.29			0.26				0.26	1.80
*M*7	0.31	0.31			0.23	0.34	0.32				0.22						0.25		1.98
*M*8		0.13			0.30	0.21			0.26		0.34			0.39	0.23				1.86
Si1					1.08			0.78			1.08	1.07							4.01
Si2								0.93	0.97				1.04	0.99					3.93
Si3	1.21		0.92	0.98			1.14												4.25
Si4		1.12	0.86			1.22				0.96									4.16
Σ_{anions}	2.07	2.00	2.02	2.13	1.95	2.08	1.96	1.95	1.83	2.13	1.93	2.17	2.13	1.91	1.06	0.90	1.15	0.87	

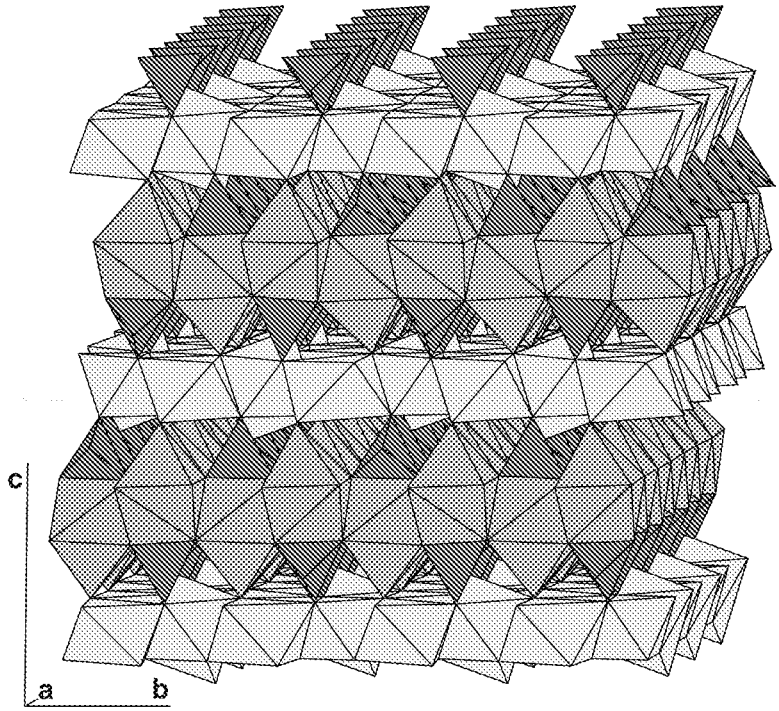

FIG. 2. The structure of roumaite, composed by the stacking of "octahedral" layers (light grey), tobermorite-like layers (grey) and disilicate groups (dark grey).

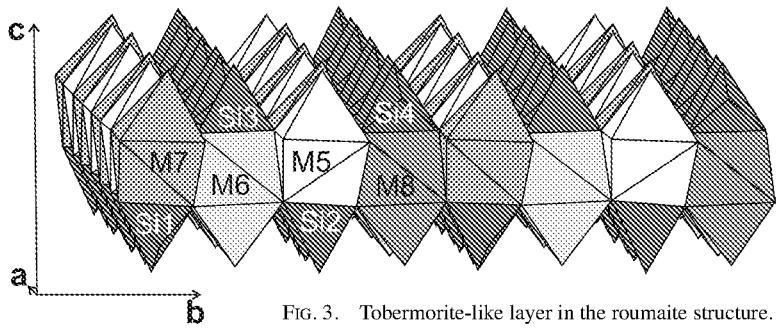

FIG. 3. Tobermorite-like layer in the roumaite structure.

geometrically similar to those of rinkite and roumaite, but with a different site-occupancy ($Ti_{0.96}Nb_{0.04}$).

The geometrical features of disilicate groups are reported in Table 7. Some bond distances are too short (*e.g.*, Si3 – O1) or too long (*e.g.*, Si1 – O8), which may be easily explained by the high structural disorder (OD character and simultaneous presence of rinkite-like domains). However, the average bond-length of the four tetrahedra is in good agreement with the average bond-length in rinkite (Galli & Alberti 1971). As in rinkite, the bridging bond in each tetrahedron in roumaite is longer than the non-bridging bonds. The bond angles in the two independent disilicate groups are 152.8° and 152.3°; these values are comparable with that found by Galli & Alberti (1971) in rinkite (155°) and that found by Sokolova & Hawthorne (2008) in nacareniobsite-(Ce), 154.9°.

The linkages between the tobermorite-like and the "octahedral" layers are achieved through the disilicate groups and the pyramidal parts of the Ca polyhedra of

the tobermorite-like layer. These apices are represented by F sites (four independent anionic sites); the chemical data suggest that these sites are occupied by three atoms of F and one OH group.

The refined occupancies are in relatively good agreement with the chemical data, taking into account the quality of the structural refinement: in fact, from the refinement, Ca, Na, REE, Nb, and Ti are respectively 3.16, 2.07, 1.22, 0.55, and 0.45 *apfu*; from chemical data, the same elements are 2.97, 2.05, 1.10, 0.69, and 0.29 *apfu*.

The crystal-chemical formula of roumaite, as suggested by structural refinement, can be written as $(Ca,Na,\square)_3(Ca,REE,Na)_4(Nb,Ti)(Si_2O_7)_2(OH)F_3$.

The OD character of roumaite

The diffraction pattern of roumaite displays, as in rinkite, features characteristic of OD structures consisting of equivalent layers. In these structures, neighboring layers can be arranged in two or more geometrically equivalent ways. The existence of different ways of connecting these layers makes it possible to obtain an infinite set of ordered (polytypes) or disordered structures, building a family of OD structures. Order–disorder theory (Dornberger-Schiff 1956, 1964, 1966, Ferraris *et al.* 2008) permits the description of the common symmetry-related properties of the whole family, focusing attention on the space transformation that converts any layer into itself (the so-called λ-POs, where PO stand for partial operation) or into the adjacent one (σ-POs).

In the case of rinkite (Ferraris *et al.*, 2008), the single layer presents symmetry *P* 2/*m* 1 (1), and the "OD groupoid family symbol" is

P 2/*m* 1 (1)

{1 $2_1/n_{2,½}$ $2_2/n_{½,1}$}

with $a_L = 7.44$, $b_L = 5.66$, $c_0 = 9.44$ Å.

In roumaite, the single layer has symmetry *C* 2/*m* 1 (1), and the set of λ and σ operations is represented by the symbol:

C 2/*m* 1 (1)

{1 $2_{½}/n_{2,½}$ $2_2/n_{½,½}$}

with $a_L = 7.473$, $b_L = 11.294$, $c_0 = 9.198$ Å.

The constant application of the operation [$-n_{2,½}$ –] gives rise to a monoclinic structure with $\mathbf{a} = \mathbf{a}_L$, $\mathbf{b} = \mathbf{b}_L$, $\mathbf{c} = 2\mathbf{c}_0 - \mathbf{a}_L/2$ (*a* 7.473, *b* 11.294, *c* 18.778 Å, β 101.7°).

In this structure, the operation σ [$-n_{2,½}$ –] becomes the total operation [– *c* –]. On the contrary, the operations [2/*m* – –] of the single layer are not valid for the whole structure. In conclusion, as the *C* centering is valid for any layer, the space group of this structure

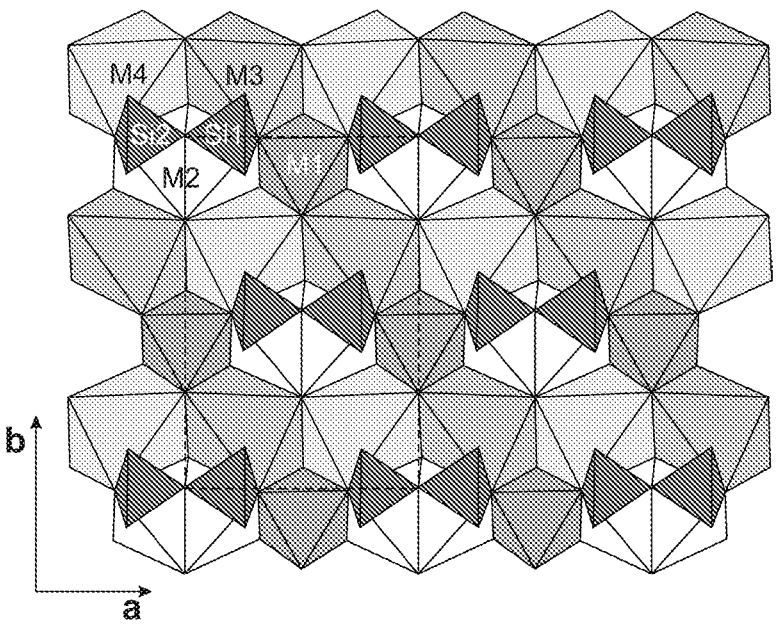

FIG. 4. "Octahedral" layer in the roumaite structure, as seen down **c***. A two-dimensional net is indicated (dashed lines).

(polytype with maximum degree of order MDO_1, Fig. 5a) is *Cc* (*C*1*c*1). The cell dimensions and space-group symmetry simply correspond to those of roumaite. The constant application of the operation [– $n_{2,-½}$ –] gives rise to the same structure-type in twin relationships with the preceding one (twin axis [100]). In fact, this kind of twinning has been observed and has been taken into account during the structure refinement.

The regular alternation of [– $n_{2,½}$ –] [– $n_{2,-½}$ –] gives rise to another main polytype (MDO_2, Fig. 5b) with pseudo-orthorhombic cell dimensions: *a* 7.473, *b* 11.294, *c* 18.396 Å. In it, the operation σ [– – 2_2] becomes the total operation [– – 2_1]. In contrast to the case of the second polytype of rinkite (Ferraris *et al.* 2008), the operation λ [2 – –] is not valid for the whole structure and does not exist the σ [– 2_1 –] operation. Therefore the structure presents the non-standard space-group symmetry *C* 1 1 2_1, with γ = 90°.

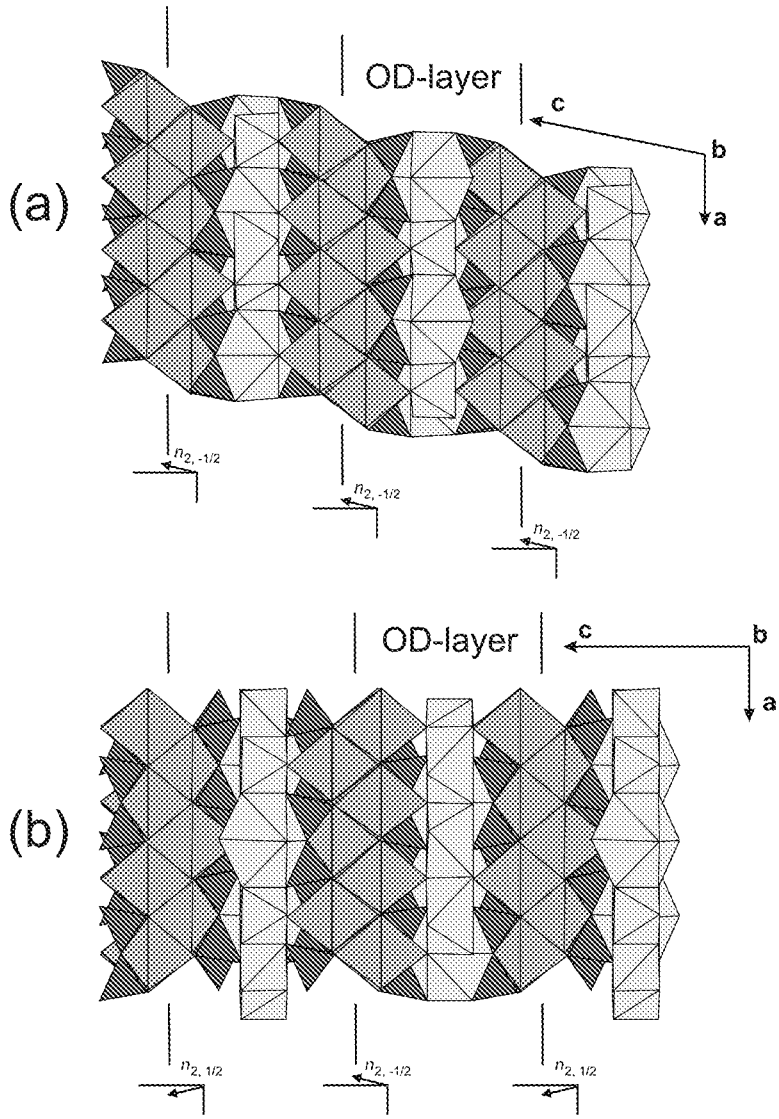

FIG. 5. MDO_1 (a) and MDO_2 (b) polytypes of roumaite. The boundaries between the OD layers, which are stacked along **c**, are indicated. The σ-POs [– $n_{2,±½}$ –] relating adjacent OD layers are also indicated.

Rinkite-like domains in roumaite and relationship to other species

Sokolova (2006) described the structure of titanium (and niobium) disilicate minerals as formed of the so-called TS (titanium silicate) blocks, which have a three-layer structure, with a central part composed by a sheet of octahedra (*O* sheet) and two adjacent sheets containing different polyhedra (*H* sheets), including the disilicate groups. Such blocks have two translation vectors, $\mathbf{t}_1$ and $\mathbf{t}_2$, with lengths $t_1 \approx 5.5$ Å and $t_2 \approx 7$ Å, and $\mathbf{t}_1 \wedge \mathbf{t}_2$ close to 90°. Sokolova (2006) defined four distinct groups of structures based upon the different types of linkage between *O* and *H* sheets. Rinkite-group minerals belong to the first group, with the disilicate groups linked to the [8]-coordinated Na site; the structure of the "octahedral" sheet of rinkite is shown in Figure 6.

Roumaite shows a different and new kind of TS block in which the $\mathbf{t}_1$ translation vector is ≈ 11.3 Å long instead of ≈ 5.5 Å. This kind of structure was also reported by Kadiyski *et al.* (2008) for dovyrenite; however, these authors resolved only the average structure of dovyrenite, suggesting the possible ordered patterns. During the present study, it was possible to solve the real structure of roumaite and to verify this new structural pattern.

Figures 4 and 6, respectively, show the "octahedral" layers of roumaite and rinkite; roumaite differs from rinkite because of a translation of **a**/2 of the two kinds of columns, alternating along [010]; in this way, the *b* parameter is doubled, and *C*-centering results.

As stated above, rinkite-like domains were detected in roumaite crystals; the relationship between these two phases in roumaite samples may be investigated by TEM studies in the future.

Roumaite is closely related to dovyrenite (Galuskin *et al.* 2007, Kadiyski *et al.* 2008), with (Nb, Ti) substituting for Zr in the cationic part, and (F, OH) replacing OH in the anionic part. As emphasized by Kadiyski *et al.* (2008) for dovyrenite, roumaite also has the same subcell of tobermorite 9 Å (riversideite). Roumaite is also linked to rinkite-group minerals and, in particular, it is chemically very similar to nacareniobsite-(Ce) (Petersen *et al.* 1989, Sokolova & Hawthorne 2008), the Nb-dominant analogue of rinkite; however, nacareniobsite-(Ce) has no extended vacancies in the sheet of octahedra. Such vacancies are instead common with mosandrite (Bellezza *et al.* 2009), in which the *M*2 and *M*3 sites are mainly empty.

It seems proper to emphasize the recurrence of the tobermorite-like modules in various structure-types. In fact, it is not only the main structural feature in all the minerals of the tobermorite group (Merlino *et al.*

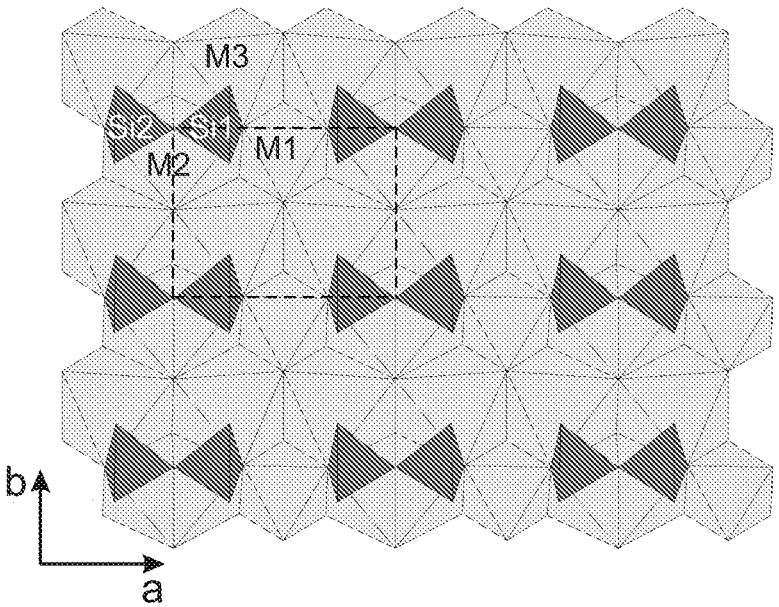

FIG. 6. "Octahedral" layer in rinkite-group minerals, as seen down **c***. A two-dimensional net is indicated (dashed lines). Sites *M*2 and *M*3 are occupied by Na and Ca in rinkite (Galli and Alberti, 1971) and nacareniobsite-(Ce) (Sokolova & Hawthorne 2008), whereas they are mostly vacant in mosandrite (Bellezza *et al.* 2009). Site *M*1 is occupied predominantly by Ti in rinkite and mosandrite, and by Nb in nacareniobsite-(Ce).

1999, Bonaccorsi & Merlino 2005) and a relevant feature in the minerals of rinkite group, in roumaite, as well as in dovyrenite, but it was also recently found as a constituting module in the structure of fukalite, $Ca_4Si_2O_6(OH)_2(CO_3)$ (Rastsvetaeva *et al.* 2005, Merlino *et al.* 2009). Finally, roumaite is the first natural phase in which the substitution $2Ca^{2+} = M^{+} + M^{3+}$ in the tobermorite-like layer occurs. This substitution was observed by Ferreira *et al.* (2003) in synthetic sodium lanthanide silicates and by Zanardi *et al.* (2006) in a sodium bismuth silicate, both with the structure type of tobermorite 11 Å.

Acknowledgements

This research received support from the SYNTHESYS Project (http://www.synthesys.info/), which is financed by European Community Research Infrastructure Action under the FP6 "Structuring the European Research Area Programme" and by MIUR through project PRIN 2007 "Compositional and structural complexity in minerals (crystal chemistry, microstructures, modularity, modulations): analysis and applications". The remarks and the suggestions of the referees, Elena Sokolova and Fernando Cámara, were helpful in improving the paper.

References

Altomare, A., Cascarano, G., Giacovazzo, C., Guagliardi, A., Burla, M.C., Polidori, G. & Camalli, M. (1994): SIR92 – a program for automatic solution of crystal structures by direct methods. *J. Appl. Crystallogr.* **27**, 435.

Bayliss, P. & Levinson, A.A. (1988): A system of nomenclature for rare-earth mineral species: revision and extension. *Am. Mineral.* **73**, 422-423.

Bellezza, M., Merlino, S. & Perchiazzi, N. (2009): Mosandrite: structural and crystal-chemical relationships with rinkite. *Can. Mineral.* **47**, 897-908.

Bonaccorsi, E. & Merlino, S. (2005): Modular microporous minerals: cancrinite–davyne group and C–S–H phases. *In* Micro- and Mesoporous Mineral Phases (G. Ferraris & S. Merlino, eds.). *Rev. Mineral. Geochem.* **57**, 241-290.

Brese, N.E. & O'Keeffe, M. (1991): Bond-valence parameters for solids. *Acta Crystallogr.* **B47**, 192-197.

Dornberger Schiff, K. (1956): On the order–disorder (OD-structures). *Acta Crystallogr.* **9**, 593-601.

Dornberger Schiff, K. (1964): Grundzüge einer Theorie von OD-Strukturen aus Schichten. *Abhandlungen der Deutschen Akademie der Wissenschaften zu Berlin, Klasse für Chemie, Geologie und Biologie* **3**, 1-107.

Dornberger-Schiff, K. (1966): *Lehrgang über OD-Strukturen*. Akademie-Verlag, Berlin, Germany.

Ferraris, G., Mackovicky, E. & Merlino, S. (2008): *Crystallography of Modular Materials*. Oxford University Press, New York, N.Y.

Ferreira, A., Ananias, D., Carlos, L.D., Morais, C.M. & Rocha, J. (2003). Novel microporous lanthanide silicates with tobermorite-like structure. *J. Am. Chem. Soc.* **125**, 14573-14579.

Galli, E. & Alberti, A. (1971): The crystal structure of rinkite. *Acta Crystallogr.* **B27**, 1277-1284.

Galuskin, E.V., Pertsev, N.N., Armbruster, T., Kadiyski, M., Zadov, A.E., Galuskina, I.O., Dzierżanowski, P., Wrzalik, R. & Kislov, E.V. (2007): Dovyrenite, $Ca_6Zr[Si_2O_7]_2(OH)_4$ – a new mineral from skarned carbonate xenoliths in basic–ultrabasic rocks of the Ioko–Dovyren Massif, northern Baikal region, Russia. *Mineral. Pol.* **38**, 15-28.

Hoffmann, C. & Armbruster, T. (1997): Clinotobermorite, $Ca_5[Si_3O_8(OH)]_2•4H_2O$ – $Ca_5[Si_6O_{17}]•5H_2O$, a natural C–S–H(I) type cement mineral: determination of the substructure. *Z. Kristallogr.* **212**, 864-873.

Kadiyski, M., Armbruster, T., Galuskin, E.V., Pertsev, N.N., Zadov, A.E., Galuskina, I.O., Wrzalik, R., Dzierżanowski, P. & Kislov, E.V. (2008): The modular structure of dovyrenite, $Ca_6Zr[Si_2O_7]_2(OH)_4$: alternate stacking of tobermorite and rosenbuschite-like units. *Am. Mineral.* **93**, 456-462.

Levinson, A.A. (1966): A system of nomenclature for rare-earth minerals. *Am. Mineral.* **51**, 152-158.

Mandarino, J.A. (1981): The Gladstone–Dale relationship. IV. The compatibility concept and its application. *Can. Mineral.* **19**, 441-450.

Mellini, M. & Merlino, S. (1979): Refinement of the crystal structure of wöhlerite. *Tschermaks Mineral. Petrogr. Mitt.* **26**, 109-123.

Merlino, S., Bonaccorsi, E. & Armbruster, T. (1999): Tobermorites: their real structure and order–disorder (OD) character. *Am. Mineral.* **84**, 1613-1621.

Merlino, S., Bonaccorsi, E. & Armbruster, T. (2000): The real structures of clinotobermorite and tobermorite 9 Å: OD character, polytypes, and structure relationships. *Eur. J. Mineral.* **12**, 411-429.

Merlino, S., Bonaccorsi, E., Grabezhev, A.I., Zadov, A.E., Pertsev, N.N. & Chukanov, N.V. (2009): Fukalite: an example of OD structure with two-dimensional disorder. *Am. Mineral.* **94**, 323-333.

Moreau, C., Ohnenstetter, D., Demaiffe, D. & Robineau, B. (1996): The Los Archipelago nepheline syenite ring-structure: a marker of the evolution of the central and equatorial Atlantic. *Can. Mineral.* **34**, 281-299.

OTWINOWSKI, Z. & MINOR, W. (1997): Processing of X-ray diffraction data collected in oscillation mode. *In* Methods in Enzymology, Volume **276**: Macromolecular Crystallography, part A (C.W. Carter Jr. & R.M. Sweet, eds.). Academic Press, New York, N.Y. (307-326).

PARODI, G.C. & CHEVRIER, V. (2004): New discoveries in nephelinites from Los Island (Republic of Guinea). 5th Int. Conf. "Mineralogy and Museums" (Paris). *Bull. Liaison, Soc. fr. Minéral. Cristallogr.* **16**(2).

PETERSEN, O.V., RØNSBO, J.G. & LEONARDSEN, E.S. (1989): Nacareniobsite-(Ce), a new mineral species from the Ilímaussaq alkaline complex, South Greenland, and its relation to mosandrite and rinkite series. *Neues Jahrb. Mineral. Monatsh.*, 84-96.

RASTSVETAEVA, R.K., BOLOTINA, N.B., ZADOV, A.E. & CHUKANOV, N.V. (2005): Crystal structure of fukalite dimorph $Ca_4[Si_2O_6](CO_3)(OH)_2$ from the Gumeshevsk deposit, the Urals. *Dokl. Earth Sci.* **405A**, 1347-1351.

SHELDRICK, G.M. (1997): SHELX–97. *Program for Crystal Structure Solution and Refinement*. Institut für Anorg. Chemie, Göttingen, Germany.

SOKOLOVA, E. (2006): From structure topology to chemical composition. I. Structural hierarchy and stereochemistry in titanium disilicate minerals. *Can. Mineral.* **44**, 1273-1330.

SOKOLOVA, E. & HAWTHORNE, F.C. (2008): From structure topology to chemical composition. V. Titanium silicates: the crystal chemistry of nacareniobsite-(Ce). *Can. Mineral.* **46**, 1333-1342.

ZANARDI, S., CARATI, A., CRUCIANI, G., BELLUSSI, G., MILLINI, R. & RIZZO, C. (2006). Synthesis, characterization and crystal structure of new microporous bismuth silicates. *Microporous and Mesoporous Materials* **97**, 34-41.

Received February 11, 2009, revised manuscript accepted February 8, 2010.